

# **Continuous-Time Simulation of Neural Synapses Using First-Order Kinetics in Xcos**

**Sumat Dhuwariya**

Department of Computer Science, VIT Bhopal University

Machine Learning

June 15, 2026

## **Abstract**

This project simulates both inhibitory and excitatory chemical synapses using the fundamental potential and current equations of the Hodgkin-Huxley (HH) model, a biological spiking neuron model that forms the mathematical foundation for Spiking Neural Networks (SNNs). The simulation was built entirely within base Scilab/Xcos using a modular, continuous-time block architecture and the concept of superblocks. To accurately model synaptic transmission, we implemented first-order kinetic equations rather than artificial square-wave pulse generators. The project implements the software simulation only. By adjusting the synaptic reversal potential, we successfully demonstrated both Excitatory Post-Synaptic Potentials (EPSP) that actively drive target neurons to spike and Inhibitory Post-Synaptic Potentials (IPSP) that suppress firing.

## 1. Introduction

The project aims to implement a continuous-time simulation of spiking neurons and chemical synapses using the foundational Hodgkin-Huxley (HH) equations within base Scilab/Xcos. We implemented membrane voltage dynamics, first-order gating kinetics ( $n$ ,  $m$ ,  $h$ ), and a synaptic bridge derived from Yu et al. [1] and Natarajan & Hasler [2] using algebraic calculators and integration superblocks. The synaptic reversal potential ( $E_{syn}$ ) is adjusted within the respective Xcos superblocks to distinguish between Excitatory Post-Synaptic Potentials (EPSPs) and Inhibitory Post-Synaptic Potentials (IPSPs), following the principles of the FPAA topology described in [3]. Instead of artificial square-wave pulse generators, neurotransmitter release is modelled through a sigmoidal activation function ( $T$ ), and temporal behavior emerges naturally from the first-order rate constants ( $\alpha$ ,  $\beta$ ) without the use of mathematical delay elements.

## 2. Problem Statement

Consider a biological neuron that operates using complex electrochemical signals; its ability to "remember" past states and communicate efficiently determines its function within the brain. Researchers modelled this behavior by utilizing the Leaky Integrate-and-Fire (LIF) model, which simplified the neuronal membrane into a basic RC (resistor-capacitor) circuit. However, circuit lacks the dynamic memory elements found in real biology. To replicate these biological functions, instead of a static leak, the Hodgkin-Huxley (HH) model uses voltage-gated channels to control the flow of current inside and outside the membrane, acting as the neuron's memory factor. Furthermore, when information is transferred from one neuron to another, it happens through a complex chemical connection. This connection either spikes the target neuron to activate it, or suppresses its voltage, referred to as Excitatory Post-Synaptic Potentials (EPSP) and Inhibitory Post-Synaptic Potentials (IPSP) respectively. In our study, we simulated these complex connections by injecting a synaptic current ( $I_{syn}$ ) governed by first-order kinetics inside Scilab/Xcos. All these concepts, along with the HH gating variables, are explained in the next section in detail.

### 3. Basic concepts related to the topic

**i. Membrane Voltage ( $V_{mem}$ ) Integrator:** The  $V_{mem}$  integrator acts as the "memory" of the cell's electrical state, starting at an initial condition of 0 mV. It continuously integrates the rate of change of the voltage ( $\frac{dV}{dt}$ ) to simulate the passage of time. As Hodgkin and Huxley established, current is carried either by charging the membrane capacity ( $C_M$ ) or by the movement of ions.

$$\frac{dV}{dt} = \frac{I_{in} - I_{Na} - I_K - I_L}{C_M} \quad (1)$$

**ii. Cellular Currents ( $I_{in}$ ,  $I_{Na}$ ,  $I_K$ ,  $I_L$ ):** The flow of electricity inside the cell is dictated by external stimuli and the biological movement of salt ions. The external stimulus ( $I_{in}$ ) acts as an artificial current injected to push the voltage past the 20 mV threshold. The ionic currents are calculated using Ohm's law: the Sodium Current ( $I_{Na} = g_{Na} \cdot m^3 \cdot h \cdot (V - E_{Na})$ ) drives the rapid spike, while the Potassium Current ( $I_K = g_K \cdot n^4 \cdot h \cdot (V - E_K)$ ) pulls the voltage back to rest. A small Leak Current ( $I_L$ ) keeps the cell balanced at equilibrium.

**iii. Potassium Activation Gate ( $n$ ):** This variable governs the outward flow of potassium ( $K^+$ ) to counteract depolarization. It relies on four activating particles, which is why it is raised to the fourth power ( $n^4$ ) to mathematically recreate the delayed "S-shape" inflexion seen in squid axon experiments. Derived from the steady-state equation at rest ( $V=0$ ), the potassium gates are roughly 31.7% open initially:

$$n_{\infty} = \frac{\alpha_{n0}}{\alpha_{n0} + \beta_{n0}} \quad (2)$$

the continuous opening and closing of these gates is governed by the differential equation:

$$\frac{dn}{dt} = \alpha_n(1 - n) - \beta_n n \quad (3)$$

For excitability test, the equation 3 was re-introduced with a  $\tau_{scale}$  in denominator of R.H.S for Bifurcation.

$$\frac{dn}{dt} = \frac{\alpha_n(1-n) - \beta_n n}{\tau_n} \quad (4)$$

Following Yu et al. (2011), the parameter ‘tau\_scale’ was introduced to scale the potassium activation time constant ( $\tau_n$ ). Under baseline conditions (tau\_scale = 1.0), the Hodgkin-Huxley neuron exhibits Class 2 excitability, characterized by a finite onset firing frequency. Increasing the parameter to tau\_scale = 3.0 slows potassium activation, increases the refractory period, and produces Class 1 excitability, allowing firing to emerge from arbitrarily low frequencies. This behavior is consistent with the dynamical-systems framework described by Izhikevich, in which Class 1 excitability is associated with a Saddle-Node on Invariant Circle (SNIC) bifurcation. However, without a formal continuation analysis, the specific topological transition (such as the occurrence of a Bogdanov-Takens bifurcation) cannot be established directly from the simulations alone.

**iv. Sodium Activation Gate ( $m$ ):** The  $m$  gate triggers the upward spike of the action potential and requires three particles to activate ( $m^3$ ). Crucially, its rate constants ( $\alpha_m$ ) are nearly 10 times faster than those of the  $n$  gate, allowing positive sodium to rush into the cell before potassium can counteract it. At  $V=0$ , its resting state is calculated to be roughly 5.2% open.

**v. Sodium Inactivation Blocker ( $h$ ):** Unlike potassium, sodium conductance is transient; it shuts itself off. The  $h$  gate is a slow-moving particle that plugs the sodium channel shortly after the  $m$  gates open, forcing the voltage to peak and fall. Derived from its steady-state equation at rest, this blocking "plug" is initially 59.6% open.

**vi. Continuous-Time Block Architecture:** The Xcos superblock relies on a continuous feedback loop between algebraic calculators and integrators. The sci\_func blocks act as instantaneous calculators, receiving the current voltage to output the instantaneous derivatives( $\frac{dV}{dt}$ ,  $\frac{dn}{dt}$ , etc.). The integrator blocks receive these rates of change and step the simulation forward in continuous milliseconds, looping the newly integrated values back into the algebra blocks to draw the action potential.

**vii. Pre-Synaptic Trigger & Neurotransmitter Release ( $T$ ):** Biological synapses do not act as perfect binary switches; they release chemicals in a physical wave. The software model utilizes a continuous sigmoidal function:

$$T = \frac{1}{1 + \exp\left(\left(-V_{pre} - V_{th}\right)/K_p\right)} \quad (5)$$

his creates a mathematically smooth, steep gradient from 0 to 1, mimicking a physical wave of neurotransmitters flooding the synaptic cleft when the pre-synaptic neuron ( $V_{pre}$ ) fires.  $K_p$  is set as 5 units, because it's a standard value.

**viii. Synaptic Gating Kinetics ( $s$ ):** The opening and closing of synaptic channels are governed by first-order kinetics. The continuous state of the synapse ( $s$ ) is mathematically derived by multiplying a channel opening rate ( $\alpha$ ) by the presynaptic neurotransmitter presence ( $T$ ) and subtracting a closing decay rate ( $\beta$ ).

$$\frac{ds}{dt} = \alpha \cdot T \cdot (1 - s) - \beta \cdot s \quad (6)$$

To simulate fast excitatory transmission, the model utilizes AMPA receptor kinetics ( $\alpha=1.1$ ,  $\beta=0.19$ ), which produce a rapid,  $\sim 5$  ms response. Conversely, neural suppression is modeled using GABA receptor kinetics ( $\alpha=0.5$ ,  $\beta=0.1$ ), yielding a slower, lingering inhibitory effect. The final current injected into the post-synaptic neuron is then scaled by the maximum synaptic conductance ( $g_{syn}$ ). Due to the driving force asymmetry inherent in the Hodgkin-Huxley convention, this conductance is asymmetrically tuned: AMPA requires only a small weight ( $g_{syn}=0.2$ ) to act as a threshold trigger, whereas GABA requires a larger conductance ( $g_{syn}=1.0$ ) to act as a current sink and successfully suppress action potentials. This continuous integration accurately models the asymmetric "triangle ramp" of post-synaptic current observed in modern hardware implementations.

**ix. Synaptic Current ( $I_{syn}$ ) & Target Response:** The final synaptic current injected into the target neuron is calculated as  $I_{syn} = g_{syn} \cdot s \cdot (E_{syn} - V_{post})$ . By flipping the voltage subtraction, the equation inherently pre-calculates the negative sign required by the

main membrane equation. Setting the reversal potential to Potassium ( $E_{syn}=-12.0$ ) creates an Inhibitory synapse (IPSP), while setting it to Sodium ( $E_{syn}=115.0$ ) creates an Excitatory synapse (EPSP).

### Some Constants and Assumptions:

The foundational constants for the neuronal membrane are directly derived from Hodgkin and Huxley's original 1952 experiments on the giant squid axon. In their relative voltage scale, the resting potential is set to 0 mV.

- **Maximum Conductances ( $g$ ):** Represent the total density of ion channels on the membrane.  $g_{Na}=120$  mS/cm<sup>2</sup>,  $g_K=36$  mS/cm<sup>2</sup>, and  $g_L=0.3$  mS/cm<sup>2</sup> (Leak).
- **Reversal Potentials ( $E$ ):** The equilibrium voltage where the net flow of a specific ion is zero, calculated biologically via the Nernst equation.  $E_{Na}=115$  mV (Drives the voltage up/depolarization),  $E_K=-12$  mV (Drives the voltage down/hyperpolarization), and  $E_L=10.613$  mV (Maintains the resting state).

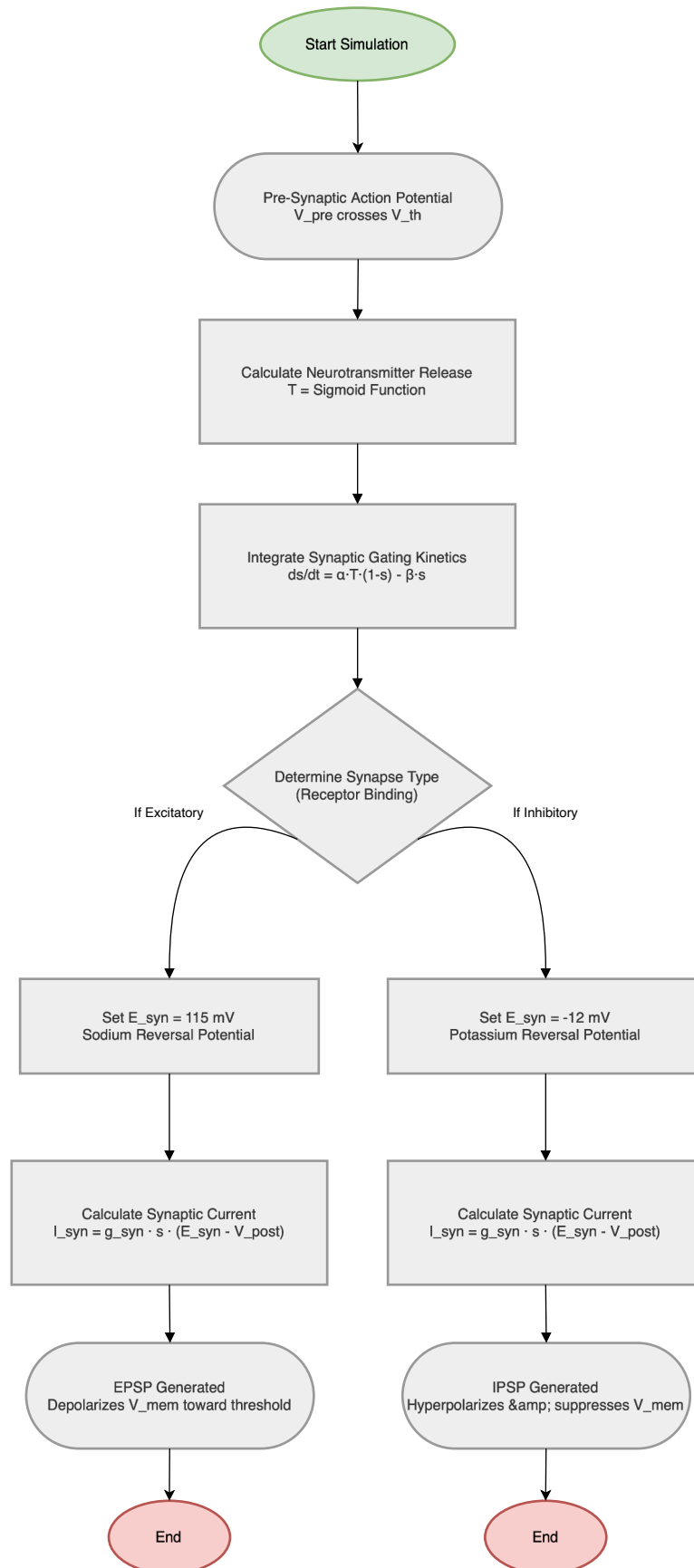
**NOTE:** The voltage used in our case study is negative, as we followed the HH's convention. The initial conditions for the integrators represent the steady-state at rest ( $V=0$ mV). At steady-state, the rate of change is zero ( $dx/dt=0$ ), leading to the derivation:

$$x_{\infty} = \frac{\alpha_{x0}}{\alpha_{x0} + \beta_{x0}} \quad (7)$$

- **Potassium Activation ( $n_0$ ):** 0.317 (Gates are ~31.7% open at rest).
- **Sodium Activation ( $m_0$ ):** 0.052 (Gates are ~5.2% open at rest).
- **Sodium Inactivation ( $h_0$ ):** 0.596 (Blocking plug is ~59.6% open at rest).

The threshold voltage  $V_{th}$  was 20mV due to neuroscience conventions, according to HH the minimum external current required should be greater than 6.3  $\mu$ A/cm<sup>2</sup> (we used 6.5 $\mu$ A/cm<sup>2</sup>), if you want to change the value, change the CONST\_m block inside the Xcos diagram. The summation block and constant was used between synapse and neuron superblocks, because to show that neurons are actively receiving independent current or no current along with injected  $I_{syn}$ .

## 4. Flowchart/Xcos Diagram





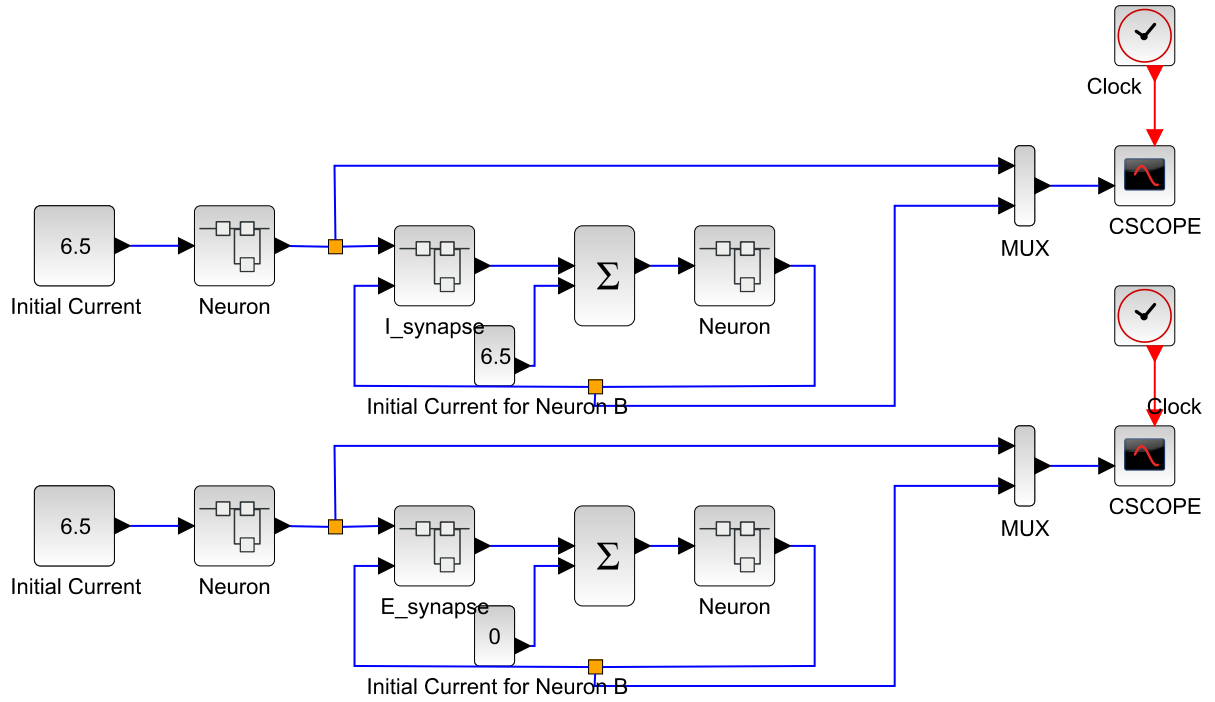


**Figure 1:** Figure1 is our Xcos diagram with superblocks, Neuron, I\_synapse, E\_synapse, some CONST\_m (constant) blocks, Mux, CSCOPE, and CLK (clock)

### Blocks:

**1) Neuron:** On the right, the main 'sci\_func' block receives the current membrane voltage ( $V_{mem}$ ) alongside the states of three biological gating variables: the potassium activation gate ( $n$ ), the fast-acting sodium activation gate ( $m$ ), and the slow sodium inactivation blocker ( $h$ ). Utilizing these inputs and initial current ( $I_{in}$ , or zap current in neuroscience), it calculates the distinct cellular currents ( $I_{na}$ ,  $I_K$ ,  $I_L$ ) and computes the instantaneous derivatives ( $\frac{dV}{dt}$ ,  $\frac{dn}{dt}$ ,  $\frac{dm}{dt}$ ,  $\frac{dh}{dt}$ ) governed by equation 1. These calculated rates of change are passed to the four integrator blocks (denoted by the  $\int$  icon) on the left. Acting as the cell's electrical memory, these integrators step the simulation forward in milliseconds from their resting conditions ( $V_{mem}=0$ ,  $n=0.317$ ,  $m=0.052$ ,  $h=0.596$ ). The newly integrated, real-time variables are then continuously looped back into the inputs of the 'sci\_func' blocks.

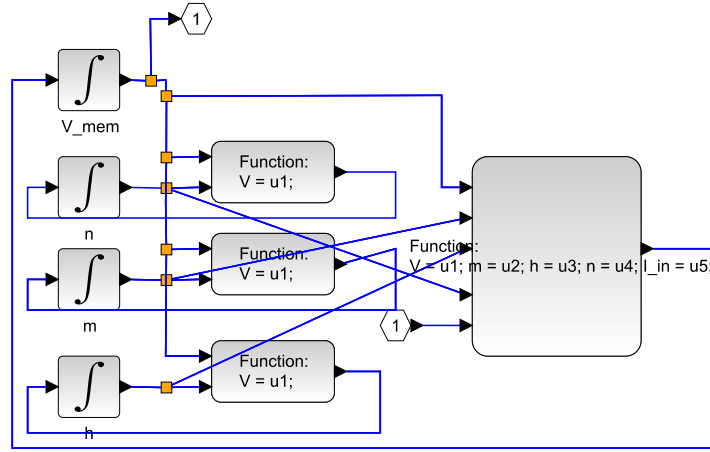


**Figure 2: Neuron Superblock**

**2) Synapse Blocks:** The Synapse superblock acts as a bridge connecting two independent HHneurons. The central sci\_func block receives three inputs: the pre-synaptic voltage ( $V_{pre}$ ), the post-synaptic voltage ( $V_{post}$ ), and a continuous feedback signal. It processes these inputs to compute a two-value array that is immediately split by a DEMUX block; the top signal outputs the rate of change for the channels ( $ds/dt$ ), which is routed through an integrator block to continuously update the s state and feed it back into the loop, while the bottom signal outputs the final computed synaptic current ( $I_{syn}$ ) that will be injected into the post-synaptic neuron.

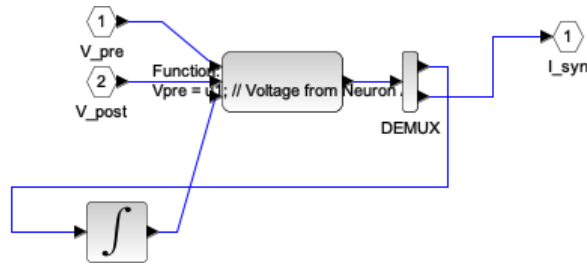


**Figure 3: Synapse Superblock**

## 5. Software/Hardware used

**Operating System:** macOS 26.3.1 (25D2128)

**Scilab Version:** 2026.1.0

**Toolboxes Used:** Base Scilab/Xcos

**Hardware:** Apple Silicon M3 processor, 8GB RAM

## 6. Procedure of execution

- Install **Scilab** (v2026.1.0 or equivalent) and place all project files in the current working directory.
- **Primary simulation:** Run Synapse.xcos.
- Open Synapse.xcos → Double-click either I\_synapse or E\_synapse → Open the internal sci\_func block → Edit the parameter g\_syn in the Scilab code.

Synapse Block	g_syn Value	Effect
I_synapse	> 1.0	Strongly suppresses Neuron B
I_synapse	< 1.0	Weakens suppression of Neuron B
E_synapse	> 1.0	Reduces Neuron A spiking due to stronger excitatory current
E_synapse	0.2–0.5	Produces smooth, regular spiking in Neuron A

- You may also vary the **zap current** in the Constant block (recommended range:  $\geq 6.3$  units [4]).
- For excitability experiments: Open Excitability.xcos -> Go to **Simulation** → **Set Context** and locate tau\_scale -> Set tau\_scale = 1.0 for **Class 2** excitability (default), increasing from 1.0 or more will show **Class 1** behavior (**Recommended:** 3.0). Run 'run\_classes.sce' and wait a few seconds for completion. Inspect the generated plots and frequency .txt file.

**Note:** All Hodgkin–Huxley dynamics, AMPA/GABA synaptic gating, and excitability bifurcation analyses were implemented from scratch in base Scilab/Xcos, without external neuroscience simulators or specialized biological toolboxes.

## 7. Implemented and Non-Implemented

Implemented	Non-Implemented
HH neuron [4] and the temperature factor convention	Bursting dynamics in [1]
First-order synaptic kinetics [1]	Calcium integrator in [1]
EPSP and IPSP tonal spiking and chemical synapses [2]	FPAA hardware realization in [3] and controlling synapses using Bias current
Controlled the synapses by $\alpha, \beta$ rates in [2]	Large neural networks in [2] and [3]
Excitability transitions [1]	Reconfigurability and parameter tuning by silicon chips in [2] and [3]

As noted by [1], tonic bursting is highly sensitive to the tuning of the calcium recovery conductance ( $g_w$ ). Since our study focuses on isolated EPSP and IPSP interactions, this parameter was considered outside the scope of the present work. Moreover, the bursting behavior reported in [1] was achieved using a reduced model that replaces the classical potassium n-gate with a slow recovery variable. To preserve biological fidelity, we retained the complete four-variable Hodgkin-Huxley formulation [4] and extracted only the relevant first-order synaptic kinetics from [1].

Although the primary objective of this project is synaptic transmission, we also validated the neural excitability dynamics described in [1] by applying a current ramp and examining both excitability classes through scaling of the potassium activation time constant ( $\tau_{scale}$ ) [4]. The baseline Hodgkin-Huxley model naturally exhibits Class 2 excitability ( $\tau_{scale} = 1.0$ ). Increasing  $\tau_{scale}$  to 3.0 slows potassium activation, allowing the neuron to generate low-frequency action potentials and thereby exhibit Class 1 excitability. Values below  $\tau_{scale} = 1.0$  were not explored because pushing the classical

equations beyond their biological operating range can introduce stiff ODE numerical instability. Our simulations operate on biological timescales, in contrast to the accelerated and physically scaled hardware measurements reported in [1]. Additionally, we adhered to the original thermodynamic conditions of the 1952 squid axon experiments [4]. By simulating the nominal Hodgkin-Huxley equations at  $T = 6.3\text{ }^{\circ}\text{C}$  (where the temperature scaling factor  $\phi = 1$ ), uniform scaling across all gating variables is preserved, enabling consistent measurement of synaptic and excitability dynamics. Comparison with the FPAA results showed qualitatively similar synaptic behavior, although exact numerical agreement is not expected because the reference system employs hardware-specific parameters and transistor-level circuitry, whereas our implementation uses biological Hodgkin–Huxley equations in a software simulation environment. While larger network behaviors such as Winner-Take-All architectures could be constructed by interconnecting multiple neuron blocks, the scope of this study was limited to synaptic transmission between two neurons.

Below is our Xcos diagram for validating the Excitability, the explanation regarding Neuron superblock is in next section, we used experimental values for current ramp:

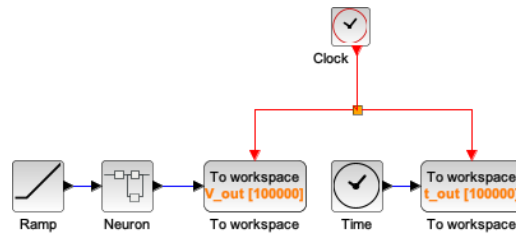


**Figure 4:** Neuron Excitability Diagram, two separate To workspace blocks were used to calculate both the time and voltage.

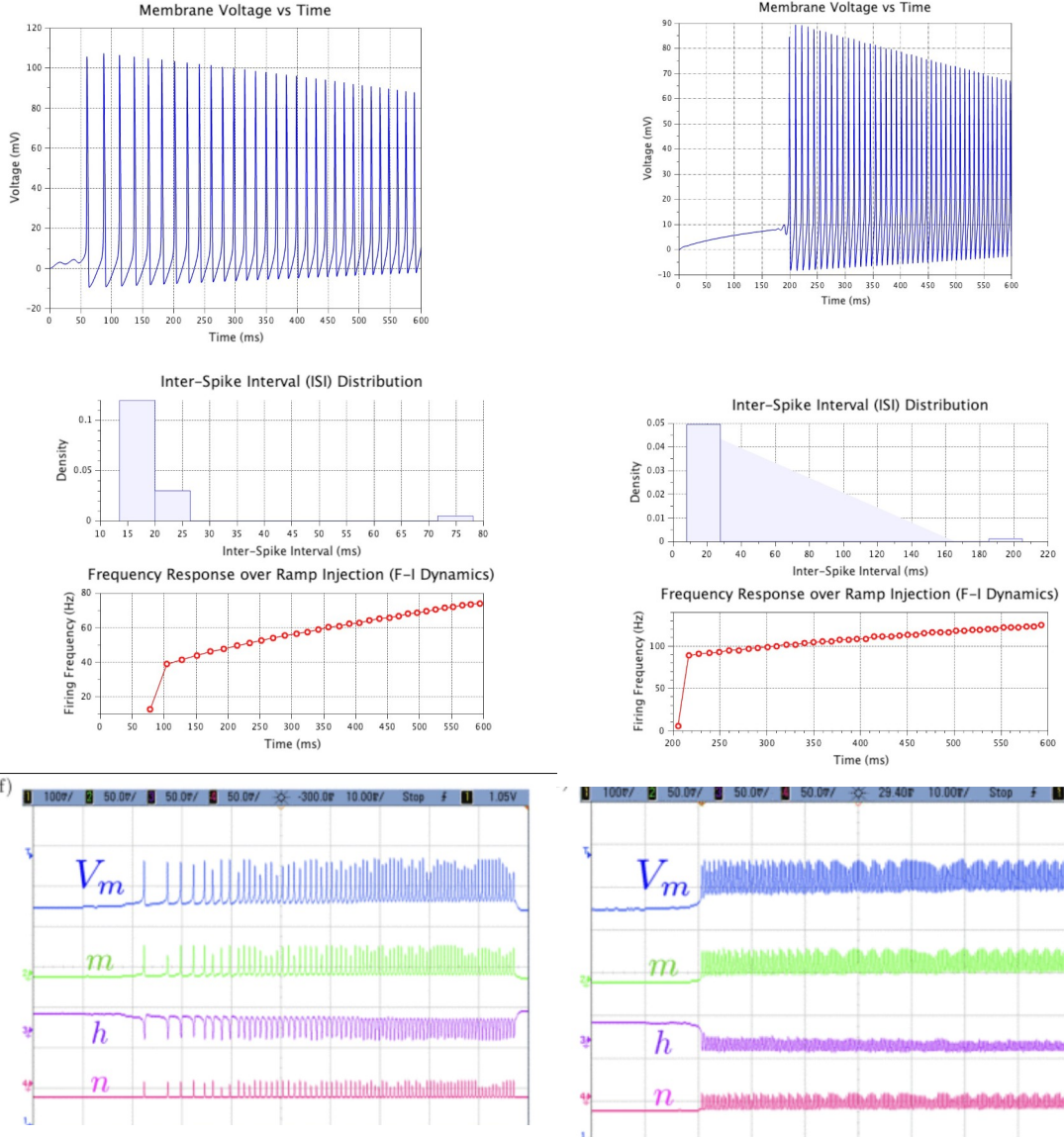


**Figure 5:** Scaling  $\tau_{scale}$  under identical ramp currents demonstrated both excitability classes [1]. Class 1 smoothly scaled from 12.8 Hz to 64.5 Hz, acting as a continuous stimulus encoder. Conversely, Class 2 exhibited prolonged resistance before abruptly jumping to 88.4 Hz, producing the rigid, densely packed spikes (shorter ISIs) characteristic of a Hopf bifurcation.

(**Note:** The values might not match with the paper due to different context in [1], but our approach is showcasing the same phenomena)

## 8. Result

The Xcos simulation was executed over a 100 ms timeframe to observe the interactions between two independent HH neurons. By changing the synaptic reversal potential ( $E_{syn}$ ), the model demonstrated both excitatory and inhibitory trans-membrane effects without the use of artificial delays or discrete logic gates. In both the graphs you will observe that a spike first goes upwards, then dips towards -12mV, it is because when a neuron spikes, it opens slow-acting Potassium ( $K^+$ ) channels to bring the voltage back down to rest. Eventually, the  $K^+$  channels finally close. Once they shut, your constant current is able to grab hold of the voltage and slowly push it back up toward the 20mV threshold to trigger the next spike.

### i. Excitatory Post-Synaptic Potential (EPSP) Validation

In this configuration, the pre-synaptic neuron (represented by the black line) is supplied with a constant current, forcing it into a state of continuous, rhythmic firing. The  $E_{syn}$  is set to 115 mV.

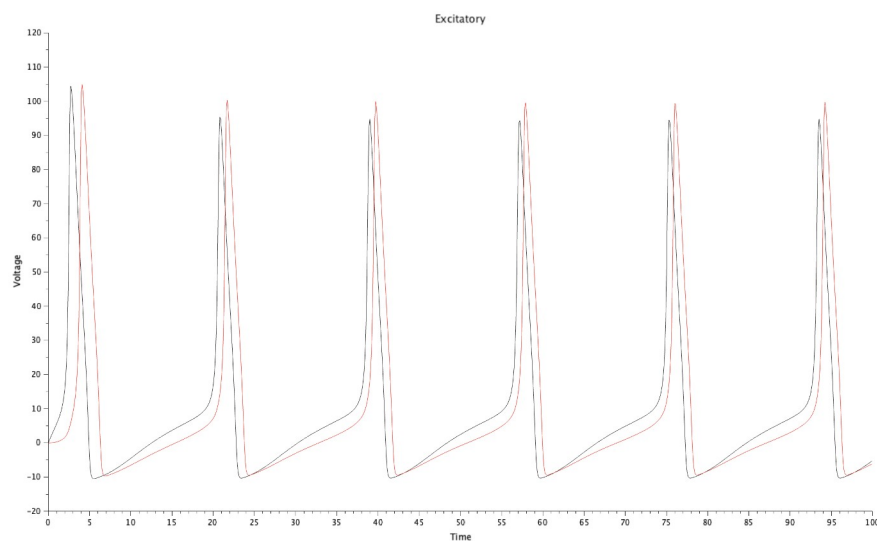


**Figure 6:** Excitatory Synapse

As the pre-synaptic voltage spikes and crosses the threshold, the continuous sigmoidal function simulates a wave of neurotransmitters opening the post-synaptic receptor channels. This influx of positive synaptic current depolarizes the target neuron (represented by the red line), actively forcing it past the 20 mV threshold and triggering a corresponding action potential. The peaks of the black and red spikes have a gap that represents the physical time required for first-order gating kinetics to calculate the transmission across the synaptic cleft. Eventually, peak of red

is slightly bigger than black, as both the  $I_{syn}$  and external current are acting.

## ii. Inhibitory Post-Synaptic Potential (IPSP) Validation

For this test, the  $E_{syn}$  was set to  $-12$  mV.

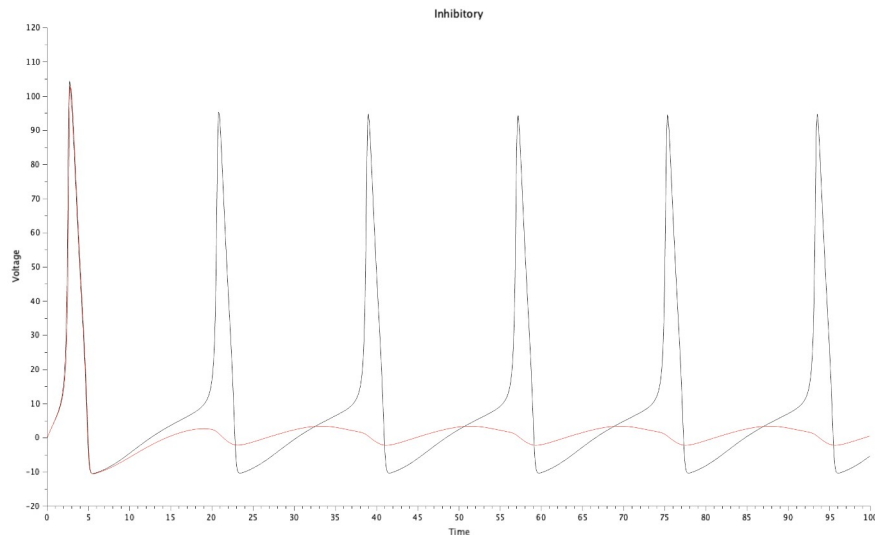


**Figure 7:** Inhibitory Synapse

Initially both fired with same peak, as they were provided with same current. The target neuron (red line) is actively prevented from reaching the required 20 mV threshold. Each time the pre-synaptic neuron fires, the resulting wave of neurotransmitters opens the inhibitory channels, injecting a negative current that drags the target neuron's membrane potential downward into a hyperpolarized state. As seen in the graph, the red line is continuously suppressed. If you will increase the initial current of post-synaptic neuron, more than pre-synaptic neuron, for values above 9 units, the peaks will be high 2-3 times and then are suppressed, if you will increase more the suppression is affected.



## 9. References

- [1] T. Yu, T. J. Sejnowski, and G. Cauwenberghs, "Biophysical neural spiking, bursting, and excitability dynamics in reconfigurable analog VLSI," IEEE Transactions on Biomedical Circuits and Systems, vol. 5, no. 5, pp. 420-429, Oct. 2011.
- [2] A. Natarajan and J. Hasler, "Hodgkin-Huxley neuron and FPAA dynamics," IEEE Transactions on Biomedical Circuits and Systems, vol. 12, no. 4, pp. 918-926, Aug. 2018.
- [3] A. Natarajan and J. Hasler, "Implementation of synapses with Hodgkin Huxley neurons on the FPAA," in 2019 IEEE International Symposium on Circuits and Systems (ISCAS), Sapporo, Japan, May 2019, pp. 1-5.
- [4] A. L. Hodgkin and A. F. Huxley, "A quantitative description of membrane current and its application to conduction and excitation in nerve," J. Physiol., vol. 117, pp. 500-544, 1952.